URSI GASS 2021, Rome, Italy, 28 August - 4 September 2021

An Experimental Study on Electromagnetic Time Reversal Focusing Property in Mismatched Media

Zhaoyang Wang(1), Hamidreza Karami(2), Adrian Löwenstein(1), Saeed Rahimi(3), Parisa Dehkhoda(3), Seyed Hossein Hesamedin Sadeghi(3), Reza Razzaghi(4), Mario Paolone(1), Marcos Rubinstein(5), and Farhad Rachidi(1)
(1) Swiss Federal Institute of Technology Lausanne (EPFL), Lausanne, Switzerland
(2) Bu-Ali Sina University, Hamedan, Iran
(3) Amirkabir University of Technology, Tehran, Iran
(4) Monash University, Melbourne, Australia
(5) University of Applied Sciences of Western Switzerland, Yverdon, Switzerland

Abstract

We present in this paper an experimental study on the focusing property of electromagnetic time reversal (EMTR) in a scattering medium, in particular when a moderate lumped mismatch between the forward- and backward-propagation media occurs. The proposed experimental set-up consists of a 26×17.5 cm^2 area, in which 20 plexiglass dielectric rods were evenly disposed in a matrix of 4×5 with a separation distance between two adjacent rods being 6.5 cm. The objective is to assess the EMTR focusing property when a limited number of rods are removed from the medium in the backward phase. The experimental analysis shows that, in the considered cases of lumped mismatched media, the original source location could still be identified using the time-reversal technique, although the focusing performance is found to be lower than that achieved in matched media.

1 Introduction

The classical applications of time reversal (e.g., in acoustics and electromagnetics) adhere to the principle of *matched media*, namely the backward-propagation medium (in the *reversed time*) is strictly identical to the one of the forward-propagation phase, namely the *direct time* [1]. However, this may not be the case in some applications related to, for instance, biomedicine or communication. Also, when locating electrical faults, since the location of the transverse branch representing the fault is unknown, multiple simulation runs are needed to satisfy the principle [2, 3]. In this regard, the concept of *mismatched* or *changing media* has emerged to describe the scenario where the time-reversed and back-injected signal, for example, acoustic or electromagnetic waves, propagates through a medium different from the one wherein it has been generated by its original source [4, 5].

Liu et al. [5] designed an experimental set-up, which consists of a number of movable dielectric rods, to study the electromagnetic time reversal (EMTR) focusing property in a highly scattering medium with a particular focus on the source localization performance in shifted mismatched media.

In this paper, we present a study, inspired by the research of Liu et al. [5], investigating the EMTR focusing property in a scattering medium. In our study, we consider moderate lumped changes in the backward phase, as opposed to [5] in which the mismatch was distributed in all the medium.

2 Proposed Experimental Set-up for Analyzing the EMTR Focusing Property in Mismatched Media

Unlike the dielectric-rod set-up in [5] wherein the rods were employed in a large quantity and distributed in an irregular pattern, we considered a compact set-up. A total of 20 rods were employed and arranged regularly between the transmitting and receiving antennas, as illustrated in Fig. 1. The objective is to assess the focusing property when a limited number of rods (1 or 2 out of 20) are removed from the medium in the backward phase. Indeed, the number of the scattering paths being substantially reduced in comparison with that of the densely-distributed rods in [5], we hypothesize that a moderate lumped mismatch between the two phases' media would not impair locating the original source and the contributions associated with the remaining rods would still render the focusing property achievable [6, 7].

The experimental set-up shown in Fig. 1 was realized in the EMC Laboratory of Amirkabir University of Technology. It was composed of a 26×17.5 cm^2 area, in which 20 plexiglass dielectric rods were evenly deployed in a matrix of 4×5 with a spacing distance between two adjacent rods being 6.5 cm. The geometrical and electrical parameters of the set-up are reported in Table 1. As illustrated in the bottom figure of Fig. 1, each rod was labeled with a coordinate (r, c) according to the row and column numbers of its location.

Two double-ridged horn antennas separated by a distance of 30 cm were used as transmitting and receiving antennas.

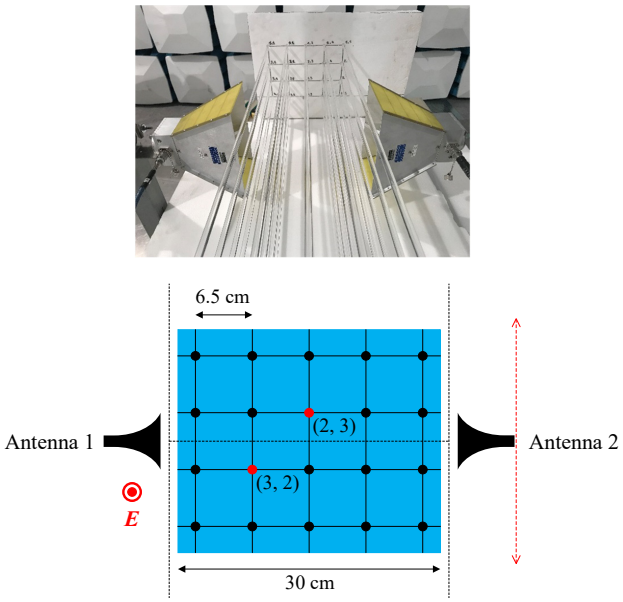

Figure 1. Dielectric-rod experimental set-up: picture (top) and schematic representation of the half-length cross-section of the rods (bottom).

Table 1. Geometrical and electrical parameters of the dielectric-rod set-up of Fig. 1

Component	Parameter	Value
Rod	Length	1 m
	Diameter	1 cm
	Relative dielectric constant	2.7
Baseboard	Relative dielectric constant	2

The center point of the transmitting/receiving antenna's aperture was aligned with the half-length cross-section of the rods. Antenna 2 (i.e., the receiving antenna) was mounted on a stepper motor and could thus be moved vertically with a precision of one centimeter.

In the forward phase, the electric field was measured by the receiving antenna in the presence of all 20 rods. While, in the backward phase, we considered the following four experimental cases (summarized in Table 2):

***Case* 0**: The forward- and backward-propagation media were matched (i.e., no rods removed),
***Cases* 1** and **2**: One rod out of 20 was removed [either $(2,3)$ or $(3,2)$, see Fig. 1],
***Case* 3**: Two rods out of 20 [$(2,3)$ and $(3,2)$, see Fig. 1] were removed.

3 Experimental Analysis

The focusing property of EMTR in the proposed lumped-type mismatched media was investigated experimentally in the frequency domain.

As illustrated in Fig. 2, in the forward phase, Antenna 1 was oriented to generating a vertically-polarized electric field. The transmission coefficient S_{21} was measured to quantify the transmitting-receiving characteristics in the frequency domain. To this end, a vector network analyzer (VNA) was used, considering the frequencies ranging from 7 to 18 GHz to intensify the interaction between the propagated fields with the rods.

Table 2. Experimental cases for the backward-propagation medium

	Case n	Rod(s) removed in the backward phase
0	Matched	None
1	Mismatched	$(2,3)$
2	Mismatched	$(3,2)$
3	Mismatched	$(2,3)$ and $(3,2)$

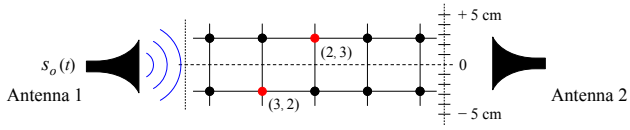

Figure 2. Schematic representation of the experimental set-up in the forward phase.

To facilitate the description, we refer to the measured S_{21}-parameter as a transfer function

$$T_n^{0,h}(f) = S_{21}(f)\,, \tag{1}$$

where 0 in the superscript stands for the height of the transmitting antenna (i.e., Antenna 1), which was fixed at $h = 0$ (the reference height). The second superscript h identifies the height of the receiving antenna (i.e., Antenna 2), which in the experiment varied from -5 cm to $+5$ cm, namely $h = -5, -4, \ldots, 0, \ldots, +4, +5$. The subscript n corresponds to one of the experimental cases proposed in Table 2 and thus it takes the following values: $0, 1, 2, 3$. For example, $T_0^{0,-1}$ represents the S_{21}-parameter being measured when the receiving antenna is at the height of -1 cm with all the rods being present (i.e., *Case* 0 of the matched media).

In view of the four experimental cases of Table 2 and 11 considered heights for the receiving antenna, a total of 44 transfer functions were measured. The measured magnitude spectrum of $T_0^{0,-1}$ is depicted in Fig. 3 as an example.

In the following analysis, we assume that the initial excitation signal $s_o(t)$ is a modulated Gaussian pulse (see its time-domain profile in the top figure of Fig. 4) given by

$$s_o(t) = \cos\left(2\pi \cdot f_c \cdot t\right) \cdot e^{-\left(t/\sqrt{2}\delta\right)^2} \tag{2}$$

with

$$\delta = 1/f_c\,, \tag{3}$$

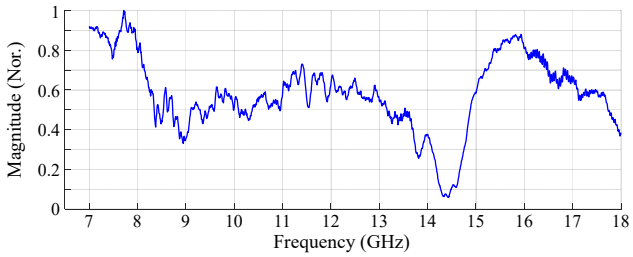

Figure 3. Normalized magnitude spectrum of the measured transfer function (i.e., S_{21}-parameter) $T_0^{0,-1}$.

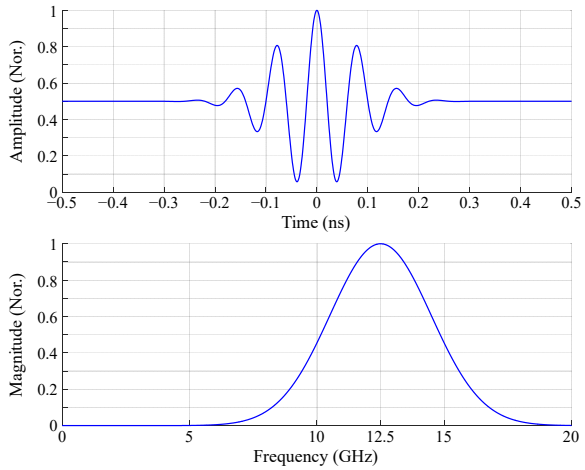

Figure 4. Morlet wavelet used as an exciting signal at the input of Antenna 1: time-domain waveform (top) and magnitude spectrum (bottom).

where f_c is the center frequency of the Gaussian function shaped magnitude spectrum of $s_o(t)$. As shown in the bottom figure of Fig. 4, a value of 12.5 GHz was assumed for f_c according to the considered frequency band ranging from 7 to 18 GHz.

The forward-phase (indicated by the superscript 'DT' as the abbreviation of *direct time*) transfer function, in which both the antennas are at the reference height $h = 0$, is given by

$$T^{\mathrm{DT}}(f) = T_0^{0,0}(f) = S_{21}{}_0^0(f). \tag{4}$$

The received signal reads in the frequency domain as

$$S^{\mathrm{DT}}(f) = T^{\mathrm{DT}}(f) \cdot S_o(f), \tag{5}$$

where, $S_o(f)$ is the Fourier transform of $s_o(t)$.

The backward propagation consists of the time-reversed copy $s^{\mathrm{DT}}(-t)$ being back injected from Antenna 2. Meanwhile, taking *Case* 3 as an example, the two rods, $(2,3)$ and $(3,2)$, are removed from the original propagative medium, as schematically described in Fig. 5.

The time-reversal operation in the frequency domain corresponds to the complex conjugate transformation:

$$S^{\mathrm{DT}*}(f) \triangleq \left[S^{\mathrm{DT}}(f)\right]^*. \tag{6}$$

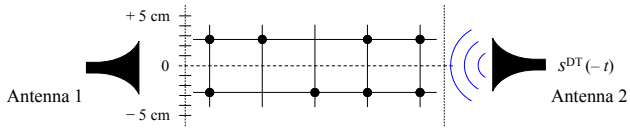

Figure 5. Schematic representation of the experimental set-up for mismatched-media *Case* 3 in the backward phase.

Thus, the frequency spectrum of the field measured by Antenna 1 in the backward phase can be calculated by

$$S_n^{\mathrm{RT}}(f,h) = S^{\mathrm{DT}*}(f) \cdot T_n^{0,h}(f), \tag{7}$$

where n and h are in the ranges defined earlier.

3.1 *Case* 0: Matched Media

Because of the low-loss medium, the field measured at the source location (specified in the present case by the reference height $h = 0$) is approximately a time-reversed copy of the original excitation [1, 8]. Thus, the source location can be identified in the frequency domain by evaluating the mean square error (*MSE*) between the source excitation and the received field in the backward phase:

$$h_o = \arg|_h \quad Min\{\, MSE(f,h)\}\,, \tag{8}$$

and

$$MSE(f,h) = \frac{1}{N} \cdot \sum_{f_{\mathrm{lower}}}^{f_{\mathrm{upper}}} \left| Nor\left\{S_n^{\mathrm{RT}*}(f,h)\right\} - S_o(f) \right|^2, \tag{9}$$

where h_o is the estimated source location (i.e., the height of Antenna 1). N is the number of samples in the frequency band ranging from $f_{\mathrm{lower}} = 7$ GHz to $f_{\mathrm{upper}} = 18$ GHz, being set to 1601 in the experiment. The normalization operation with the notation *Nor* in (9) is given by

$$Nor\left\{S_n^{\mathrm{RT}*}(f,h)\right\} = \frac{S^{\mathrm{DT}*}(f) \cdot T_n^{0,h}(f)}{\left|T_0^{0,0}(f)\right|^2}. \tag{10}$$

Figure 6 presents the calculated *MSE* metric as a function of the height of the receiving antenna for *Case* 0. As anticipated, the global minimum of the *MSE* metric in Fig. 6 for the matched-media case obviously corresponds to the original source location as a result of considering the same medium in the two propagation phases.

3.2 *Cases* 1-3: Mismatched Media

For the three considered mismatched cases defined in Table 2, the results of the *MSE* evaluations are shown in Fig. 7. It is evident that, for the present study, the number of scattering paths is limited in comparison with that of the set-up in [5] wherein a total of 750 rods were distributed with an average inter-rod spacing of 6.5 cm. In spite of that, the absence of one or two rods in the backward-propagation

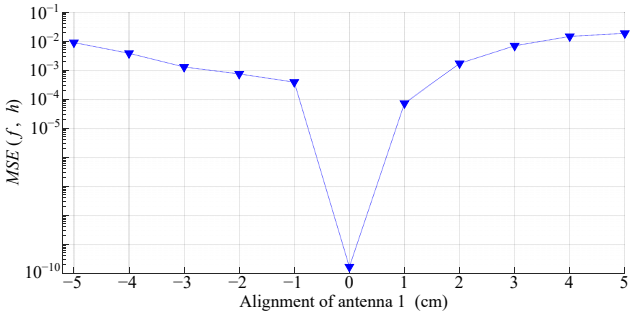

Figure 6. Mean square error metric of (9) as a function of the alignment of Antenna 1 in the backward phase for the matched-media case.

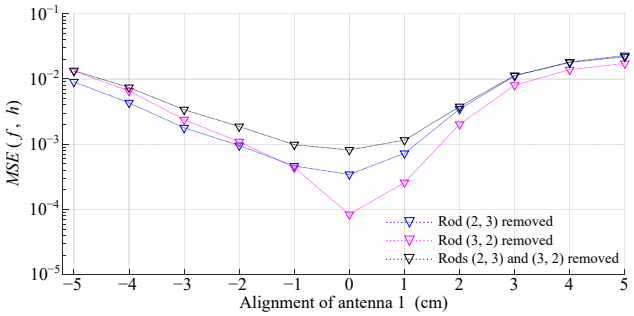

Figure 7. Mean square error metric of (9) as a function of the alignment of Antenna 1 in the backward phase for the mismatched-media cases.

medium does not dramatically compromise the EMTR focusing property. As it can be observed, the source location can still be identified by means of the *MSE* metric formulated in (9). Certainly, the focusing performance is lower than that achieved in matched media (compare Figs. 6 and 7). However, the contributions associated with the fixed rods still enable the focusing property effective.

4 Conclusion

We presented an experimental study aiming at investigating the EMTR focusing property in lumped mismatched media.

The proposed experimental set-up consisted of a total of 20 dielectric rods between two double-ridged horn antennas (e.g., transmitting and receiving antennas). The mismatched-media scenario specified in the study referred to removing a limited number of rods (1 or 2 out of 20) from the medium in the backward phase. The experiment was performed in the frequency domain using a vector network analyzer, in the frequency range from 7 to 18 GHz.

The experimental analysis confirmed that, in absence of one or two rods in the backward-propagation medium, the original source location could still be identified using the time-reversal-based metric. It goes without saying that the lumped-type modification implies a controlled mismatch between the forward- and backward-propagation media. It was observed that, as the mismatch is intensified by removing an increasing number of rods, the focusing quality can be degraded.

5 Acknowledgments

This work has been carried out within the frame of the Swiss Centre for Competence in Energy Research on Future Swiss Electrical Infrastructure (SCCER-FURIES) with the financial support of the Swiss Innovation Agency (Innosuisse-SCCER program).

References

[1] M. Fink, “Time Reversal of Ultrasonic Fields-Part I: Basic Principles,” *IEEE Transactions on Ultrasonics, Ferroelectrics, and Frequency Control*, vol. 39, no. 5, pp. 555–566, 1992.

[2] Z. Wang, R. Razzaghi, M. Paolone, and F. Rachidi, “Electromagnetic Time Reversal Similarity Characteristics and Its Application to Locating Faults in Power Networks,” *IEEE Transactions on Power Delivery*, vol. 35, no. 4, pp. 1735–1748, 2020.

[3] Z. Wang, R. Razzaghi, M. Paolone, and F. Rachidi, “Time Reversal Applied to Fault Location in Power Networks Pilot Test: Results and Analyses,” *International Journal of Electrical Power and Energy Systems*, vol. 114, p. 105382, 2020.

[4] G. Bal and R. Verástegui, “Time Reversal in Changing Environments,” *Multiscale Modeling and Simulation*, vol. 2, no. 4, pp. 639–661, 2004.

[5] D. Liu, S. Vasudevan, J. Krolik, G. Bal, and L. Carin, “Electromagnetic Time-Reversal Source Localization in Changing Media: Experiment and Analysis,” *IEEE Transactions on Antennas and Propagation*, vol. 55, no. 2, pp. 344–354, 2007.

[6] A. Codino, Z. Wang, R. Razzaghi, M. Paolone, and F. Rachidi, “An Alternative Method for Locating Faults in Transmission Line Networks Based on Time Reversal,” *IEEE Transactions on Electromagnetic Compatibility*, vol. 59, no. 5, pp. 1601–1612, 2017.

[7] Z. Wang, A. Codino, R. Razzaghi, M. Paolone, and F. Rachidi, “Using Electromagnetic Time Reversal to Locate Faults in Transmission Lines: Definition and Application of the "Mirrored Minimum Energy" Property,” in *2017 International Symposium on Electromagnetic Compatibility ,EMC EUROPE 2017*, 2017.

[8] Z. Wang, F. Rachidi, M. Paolone, M. Rubinstein, and R. Razzaghi, “A Closed Time-Reversal Cavity for Electromagnetic Waves in Transmission Line Networks,” *IEEE Transactions on Antennas and Propagation*, pp. 1–9, 2020.